Removal of pb(II)

by Fahma Riyanti

Submission date: 27-Apr-2023 03:55PM (UTC+0700)
Submission ID: 2077016405
File name: Removal_of_Pb_II_usingmolekul2020.pdf (420.05K)
Word count: 5164
Character count: 27756

MOLEKUL
www.jmolekul.com

Articles

https://doi.org/10.20884/1.jm.2020.15.2.641

Removal of Pb(II) using Hydroxyapatite from Golden Snail Shell (*Pomacea canaliculata* L.) Modified with Silica

Poedji Loekitowati Hariani*, Fahma Riyanti, Fatma, Addy Rachmat, Aldi Herbanu

Department of Chemistry, Faculty of Mathematics and Natural Science, Sriwijaya University, Palembang, Indonesia

*Corresponding author email: puji_lukitowati@mipa.unsri.ac.id

Received February 08, 2020; **Accepted** June 06, 2020; **Available online** July 27, 2020

ABSTRACT. The composites of hydroxyapatite and SiO_2 were successfully synthesized. The hydroxyapatite was prepared from golden snail shells (*Pomacea canaliculata* L). The hydroxyapatite and hydroxyapatite-SiO_2 composites were characterized using XRD, FTIR, SEM-EDS. Furthermore, hydroxyapatite and hydroxyapatite-SiO_2 composites were used to remove Pb(II) from aqueous solution. Various adsorption parameters such as pH of the solution, contact time, and initial Pb(II) concentration were used to study the adsorption process. The optimum pH of the solution for removal of Pb(II) by hydroxyapatite and hydroxyapatite-SiO_2 composite at pH 6 and contact time at 60 minutes. Both adsorbents follow the Langmuir isotherm. The maximum adsorption capacity of the hydroxyapatite-SiO_2 composite is greater compare to hydroxyapatite, respectively 135.14 and 123.46 mg/g. The pseudo-second order kinetic model had a correlation coefficient (R^2) greater than the pseudo-first order so pseudo-second order kinetic is better to describe adsorption kinetics.

Keywords: Hydroxyapatite, SiO_2, composite, adsorption, Pb(II),

INTRODUCTION

Heavy metals such as lead, nickel, lead, mercury, chromium, copper are commonly found on the surface water and groundwater. Industrial wastewater has a role in the presence of heavy metals in the environment. Heavy metals are toxic compounds for humans, other living organisms, and the environment (Samuel, Shah, Bhattacharya, Subramaniam, & Singh, 2018). In addition, heavy metals have properties that are difficult to degrade and accumulate in the body of organisms. One of the heavy metals found in industrial wastewater is lead. The presence of lead in small concentrations in water is harmful to human and aquatic animals due to accumulation in the food chain (Dong, Zhu, Qiu, & Zhao, 2010). Lead is difficult to break down naturally. Lead can have a serious impact on living organisms that trigger kidney disorders, anemia, hemolysis, liver dysfunction, and neuron cell injury (Jarup, 2003; He et al., 2019). The World Health Organization (WHO) has set permitted limits for lead in drinking water 0.01 mg/L while the US Environmental Protection Agency (US EPA) sets a maximum of 0.015 mg/L. Wastewater treatment is very important before being released into the environment.

Technologies that can be used to eliminate Pb include extraction (Tawinteung, Parkpian, Dealune, & Jugsujinda, 2005), precipitation (Kavak, 2013), membrane (Hajdu et al., 2012), electrochemical (Li et al., 2017), ion exchange (Meyers, Gottlieb, & Desilva, 2013) and adsorption (He et al., 2019). Adsorption is a method based on chemical or physical interactions between pollutants and adsorbents. This method is often used in wastewater treatment because it is effective for removing heavy metal ions, simple and inexpensive technology (Gu, Wang, Mao, Yang, & Wang, 2018; He et al., 2019). The adsorption methods are developed to obtain adsorbents that are environmentally friendly, inexpensive, abundant in availability, and large adsorption capacity.

Hydroxyapatite has the molecular formula $Ca_{10}(PO_4)_6(OH)_2$. Hydroxyapatite is a major component of human hard tissue. Synthetic hydroxyapatite is widely used for bioceramics as an adsorbent in chromatography for the separation of proteins and enzymes, methane oxidation, dehydration, and dehydrogenation of alcohol (Skwarek, 2014). It is also used in the medical field for bone and dental implants. Some literature reports that hydroxyapatite can be used to adsorb pollutants such as phenol (Lin, Pan, Chen, Cheng, & Xu, 2009), Cu (Ramesh, Ramesbabu, Gandhimathi, Nidheesh, & Kumar, 2012), Zn (Skwarek, 2014), Pb (Iconaru, Heino, Guegan, & Predoi, 2018) and Ni (Hariani, Muryati, & Said, 2019).

Hydroxyapatite can be synthesized using chemical reagents or extracted from materials containing calcium. Hydroxyapatite from biomaterials has the advantage of being biodegradable and low cost. Various biomaterials can be used as a source of

hydroxyapatite such as fish bones (Sunil, & Jagannatham, 2016), eggshells (Wu, Hsu, Hsu, Chang, & Ho, 2016), animal bones (Miecznik, Haberko, Sitarz, Bucko, & Macherzynska, 2014). Biomaterials that are also potentially used as a source of hydroxyapatite are golden snail shells. Golden snail (*Pomacea canaliculata* L) is one of the animals in Indonesia which is abundant in freshwater waters and has not been used optimally. The golden snails belong to the species of snails in Mollusca phylum, animals with soft-bodied features that are protected by hard golden shells containing calcium carbonate (Campbell, Reece, & Mitchell, 2005). Golden snails are considered as one of the pests in rice plants.

The adsorption capacity can be increased by combined hydroxyapatite with other materials to become a composite. Some researchers have combined hydroxyapatite with other materials such as hydroxyapatite/magnetite for lead removal (Dong et al., 2010), hydroxyapatite/manganoxide for lead removal (Dong, Zhu, Qiu, & Zhao, 2016), hydroxyapatite/graphene hybrid for removal of methylene blue dye (Hassan, Mohammed, Salaheldin, & El-Anadouli, 2018) and hydroxyapatite/chitosan for brilliant green dye adsorption (Ragap, Ahmed, & Bader, 2019).

In this study, hydroxyapatite was modified with silica and used to remove lead. Hydroxyapatite is prepared from golden snail shells. Silica is reported to be used to adsorb organic compounds and metal ions (Sayari, Hamoudi, & Yang, 2005; Parida, Dash, Patel, & Mishra, 2006; Dhmees, Khaleel, & Mahmoud, 2018). The influence of several parameters (pH of the solution, contact time, and initial concentration), isotherms, and kinetics were studied in this study.

EXPERIMENTAL SECTION

Materials

The golden snail shells were obtained from rice fields in the Ogan Ilir city. The chemicals reagent used includes $(NH_4)_2HPO_4$, HNO_3, NH_4OH, CH_3COOH, $PbCl_2$, NaOH, CH_3COOH, HCl, tetraethylorthosilicate (TEOS), methyltriethosilane (MTES) from Merck, Germany. The equipment in the research used UV-Vis Spectroscopy (Genesys 20), XRD Rigaku Miniflex 600, FTIR Thermo Nicolet iS10, SEM-EDS (Shimadzu AA-7000), and AAS (Shimadzu AA 7000).

Synthesis of hydroxyapatite from golden snail shell

The golden snail shell was cleaned of impurities using water and then boiled for 1 hour. The shell was separated from the meat and then dried in the sun for 1 day. The shell was crushed to the size of 100 mesh. 50 g of shell were calcined at 900 °C for 4 hours to convert the $CaCO_3$ into the CaO phase. The calcination reaction is as follows.

$CaCO_3 \rightarrow CaO + CO_2$

CaO (11.216 g) was put into a 500 mL beaker glass with 100 mL of distilled water. After that, 200 mL of 2 M nitric acid solution was added, and then the solution stirred at 600 rpm for 30 minutes at 90 °C. Subsequently, 15.84 g of $(NH_4)_2HPO_4$ was added to the solution. The pH of the solution being maintained at 9-10 by dropping NH_4OH at a rate of 1 mL/min using a burette. The solution was left to stand for 24 hours so that a precipitate formed. The precipitate obtained was filtered, then washed using distilled water. Finally, precipitate dried for 1 hour at 100 °C.

Synthesis of hydroxyapatite-SiO_2 composite

The hydroxyapatite-SiO_2 composite synthesis uses the sol-gel method (Latifi, Fathi, & Golozar, 2012). The ratio of TEOS and MTES is 1:1, the ratio of H_2O and (TEOS + MTES) is 2:1, and the ratio of water and acetic acid is 7:1. A total of 50 mL of the mixture is stirred to form a sol. Subsequently, hydroxyapatite was added as much as 5 g and stirred for 2 hours. The mixture was allowed to stand for 24 hours to form a gel. The gel was dried in an oven at 80°C for 10 hours and continued with calcination at 600°C for 1 hour. The product obtained was crushed with a mortal to obtain a size of 100 mesh.

The crystal structure of powder was analyzed using XRD in the range of 2θ at 10-80°. The functional groups were observed with FTIR at wavenumbers of 400-4000 cm^{-1}. The morphology and element content were observed using SEM-EDS.

Determination of point zero charge (pHpzc)

The measurement of pHpzc was performed based on the method reported by Jain, et al., (2018) with modification. The pHpzc of hydroxyapatite and hydroxyapatite-SiO_2 composite was conducted using 50 mL NaCl 0.01 M, the initial pH (pH_i) was adjusted from 2-10 using 0.1 M HCl and NaOH solution. The solution was added into a conical flask containing 0.2 g hydroxyapatite or hydroxyapatite-SiO_2 composite, agitated by shaker at 120 rpm for 24 h. The final pH (pH_f) of solution was measured using pH meter. The pHpzc was determined from the graph of the $\Delta pH(pH_f - pH_i)$ versus pH_i.

Batch Adsorption Process

The effect of the pH solution is carried out in the range 2-10 was determined by adding 20 mg of hydroxyapatite-SiO_2 composite to 25 mL Pb(II) solution with a concentration of 50 mg/L. HCl and NaOH 0.1 N solutions were used to adjust the pH of the solution. The contact time effect was carried out using a shaker for 0-90 minutes, while the effect of the initial concentration of Pb(II) varies from 25 to 200 mg/L. The concentration of Pb(II) after the adsorption process was determined by Atomic Absorption Spectroscopy.

RESULTS AND DISCUSSION

Characterization of Hydroxyapatite-SiO_2 composite

The XRD patterns of hydroxyapatite, SiO_2, and hydroxyapatite-SiO_2 composite are shown in **Figure 1**. Based on JCPDS No. 09-432, hydroxyapatite has 2θ major at 25.879 (002), 31.773 (211), 32.196 (112),

32.906 (300), 49.468° (213). The peak that emerged in this study is in accordance with the hydroxyapatite phase, which has 2θ at 25.91, 31.09, 32.77, 32.85, 49.59°. The main peak of silica is at 2θ=22.003° (JCPDS No. 49-1425). In this study, the peak appears in 2θ=22.25°. Some researchers obtained silica peaks at 22.5° (Dhmees, Khaleel, & Mahmoud, 2018), and 23.0° (Music, Vincekovic, & Sekovanic, 2011). The XRD pattern of the hydroxyapatite-SiO_2 composite is a combination of hydroxyapatite and silica peak, and there is no shift in the 2θ. In the ZnO-SiO_2 composite, the peak does not have a shift, but the high intensity peak depends on the SiO_2 concentration (Widiyastuti, Machmudah, Nurtono, Winardi, & Okuyama, 2017).

The FTIR spectra of hydroxyapatite, SiO_2, and hydroxyapatite-SiO_2 composite are presented in **Figure 2**. The phosphate ion (PO_4^{3-}) is a specific functional group on hydroxyapatite that can be observed at wavenumbers 900-1200 cm^{-1} for v_1 and v_2 ions. In hydroxyapatite, the group appears at wavenumbers 1087 and 1093 cm^{-1}. In hydroxyapatite-SiO_2 composite, it appears at 1098 and 966 cm^{-1}. The presence of phosphate ion is also expressed at peak characteristics (v_3 and v_4) at 563, 626, and 910 cm^{-1} for hydroxyapatite and wavenumbers of 567, 602 and 966 cm^{-1} for hydroxyapatite-SiO_2 composite (Esmaelkhanian et al., 2019). The broadband wavenumber at 2800-3600 cm^{-1} indicates the presence of a hydroxyl group that can be found in all spectra (Balamurugan, Kannan, & Rajeswari, 2013). FTIR spectra of SiO_2 shows Si-O (δ) bonds at wavenumber 464 cm^{-1} for Si-O-Si (v_{sim} and v_{ass}) and at wavenumber 806 and 1064 cm^{-1}. The same bonds in hydroxyapatite-SiO_2 composite appear in 464, 806, and 1066 cm^{-1} (Ferreira, Santos, Bonacin, Passos, & Pocrifka, 2015).

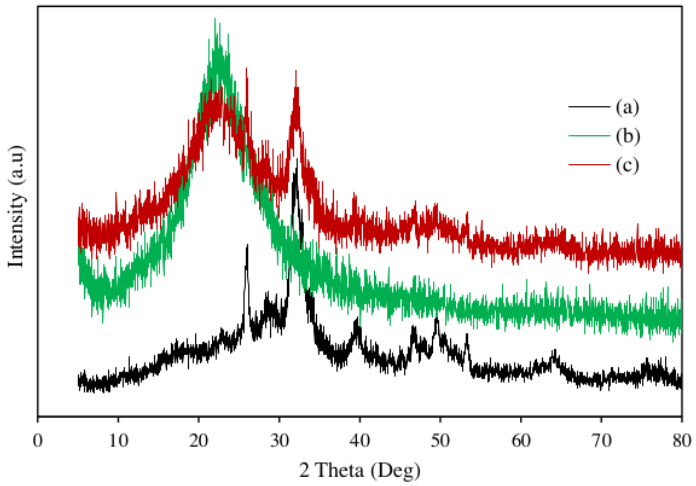

Figure 1. X-ray diffraction of (a) Hydroxyapatite (b) SiO_2 and (c) Hydroxyapatite-SiO_2 composite

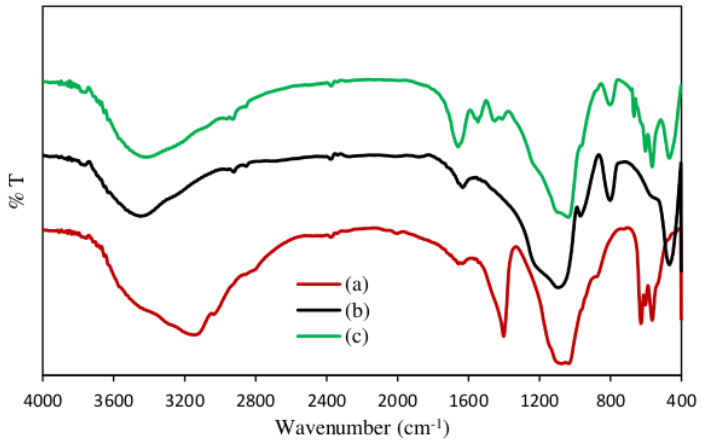

Figure 2. Spectra FTIR of (a) Hydroxyapatite (b) SiO_2 and (c) Hydroxyapatite-SiO_2 composite

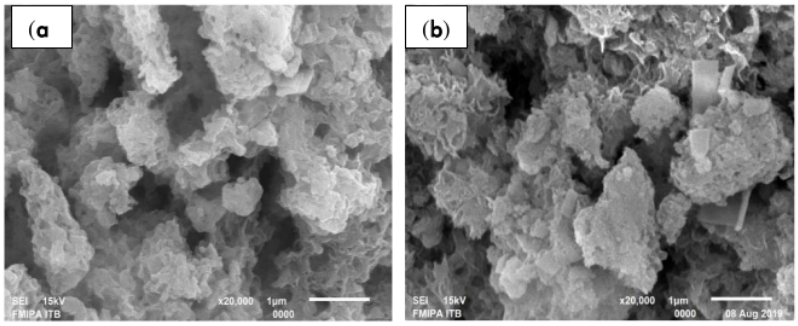

Figure 3. Morphology of (**a**) Hydroxyapatite and (**b**) Hydroxyapatite-SiO_2 composite

Table 1. The composition of the element hydroxyapatite and hydroxyapatite-SiO_2 composite

Elements (%)	Hydroxyapatite	Hydroxyapatite-SiO_2 composite
O	63.28	58.17
P	11.79	10.33
Ca	24.93	22.16
Si	-	9.34

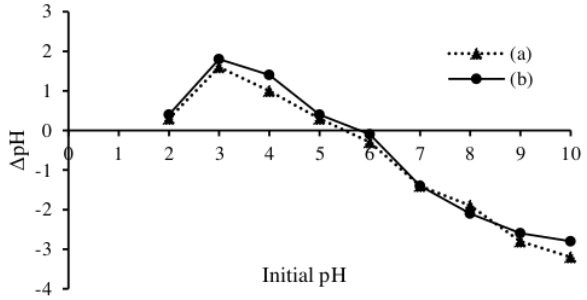

Figure 4. pHpzc of (a) Hydroxyapatite and (b) Hydroxyapatite-SiO_2 composite

The morphology of hydroxyapatite appears to have pores indicated by holes on the surface, while hydroxyapatite-SiO_2 composite has a denser surface with addition of other particles on the surface (**Figure 3**). The hydroxyapatite has a Ca/P molar ratio of 1.64, similar to a theoretical molar ratio of 1.67. The success of the synthesis is shown by the addition of Si elements in the hydroxyapatite-SiO_2 composite, as shown in **Table 1**.

pHpzc was measured to determine the charge for an adsorbent surface or isoelectric point. The surface of the adsorbent is positively charged if the pH of the solution < pHpzc and negatively charged if the pH of the solution > pHpzc (Kausar et al., 2019). The pHpzc of hydroxyapatite and hydroxyapatite-SiO_2 composite were obtained shown in **Figure 4**. pHpzc of hydroxyapatite and hydroxyapatite-SiO_2 composite were 5.5 and 5.8, respectively.

Effect of the pH solution

The pH of the solution affects the adsorption capacity of hydroxyapatite-SiO_2 to Pb ions. The surface charge of the adsorbent is affected by the pH of the solution (Kalaivani, 2014). The pH of the solution in the adsorption process was studied at range 2-10 using 25 mL of 50 mg/L Pb(II) solution. **Figure 5** shows that % removal of Pb(II) increases with increasing the solution pH and optimum % removal at pH 6. The competition between H^+ and Pb^{2+} at lower pH decreased the percentage removal. At pH of the solution > pHpzc, the negatively charged of the adsorbent. The adsorption process is effective because the adsorbent attracts Pb^{2+}, which have a positive charge. Meanwhile, at pH 8, the presence of OH^- caused Pb in solution to form $Pb(OH)_2$, $Pb(OH)_3$ and $Pb(OH)^+$ which reduced Pb^{2+} absorbed by hydroxyapatite and hydroxyapatite-SiO_2 composite (Xu, Tan, Chen, & Wang, 2008). Another study investigated that the precipitate of $Pb(OH)_2$ is formed at pH 7.5 (Le et al., 2019). The % removal of Pb(II) using hydroxyapatite-SiO_2 composite is greater than hydroxyapatite.

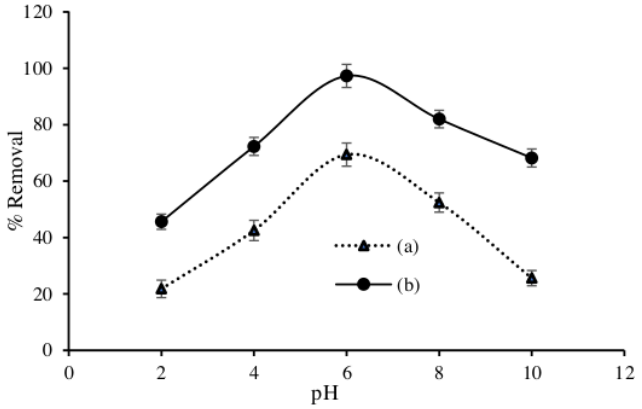

Figure 5. Effect of the pH solution on the removal of Pb(II) by (**a**) Hydroxyapatite and (**b**) Hydroxyapatite-SiO_2 composite.

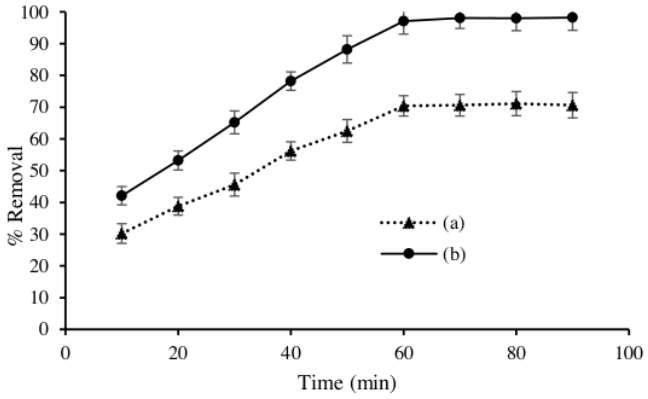

Figure 6. Effect of the contact time on the removal of Pb(II) by (a) Hydroxyapatite and (b) Hydroxyapatite-SiO_2 composite

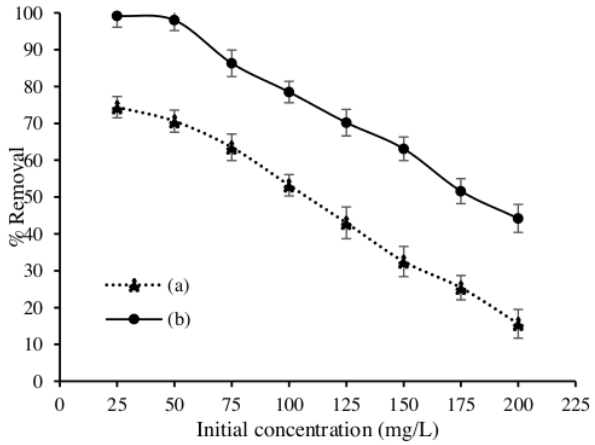

Figure 7. Effect of initial concentration on the removal of Pb(II) by (a) Hydroxyapatite and (b) Hydroxyapatite-SiO_2 composite

Effect of the contact time

The contact time in the adsorption process was studied using 25 mL of 50 mg/L Pb(II) solution at pH 6 with the amount of adsorbent 20 mg. At the contact time of 0-60 minutes, an increase in the removal of Pb(II) was observed. The % removal of Pb(II) optimum at the contact time of 60 minutes for hydroxyapatite and hydroxyapatite-SiO_2 composite (**Figure 6**). The removal of Pb(II) in using hydroxyapatite is 70.4 %, and hydroxyapatite-SiO_2 composite is 97.1 %. Thus, the presence of SiO_2 in the hydroxyapatite increases the removal of Pb(II).

Effect of initial concentration

The initial concentration of Pb (II) was investigated in the range 25-200 mg L with 25 mL, pH of the solution 6 and amount of adsorbent 20 mg. **Figure 7** shows that the initial concentration effects on the removal of hydroxyapatite and hydroxyapatite-SiO_2 composite on Pb(II). The removal of Pb(II) decreases with increasing Pb(II) concentration. The optimum removal of Pb(II) at a concentration of 25 mg/L. The amount of adsorbent remains constant, while the amount of Pb(II) concentration increases. As a result, the removal of Pb(II) decreases. The same adsorption pattern was obtained by Farghali, Bahgat, Allah, and Khedr (2013) using copper oxide nanostructure on the adsorption of Pb(II).

Adsorption Isotherm

Adsorption isotherm was determined using Pb(II) concentrations in the range of 50-200 mg/L at a constant temperature and pH. In general, adsorption isotherms explains the relationship between the amount of substance absorbed per unit mass of adsorbent (Farghali et al., 2013). Two adsorption isotherm models are used namely Langmuir and Freundlich isotherms. The equation of the Langmuir and Freundlich isotherms expressed by the equation:

$$\frac{C_e}{q_e} = \frac{1}{q_m b} + \frac{C_e}{q_m} \quad (1)$$

$$\log q_e = \log k_f + \frac{1}{n} \log C_e \quad (2)$$

Where C_e (mg/L) and q_e (mg/g) are a concentration of Pb and amount of adsorbed at equilibrium, q_m (mg/g) and b represent the maximum adsorption capacity and coefficient of Langmuir is obtained from slope and intercept of the linear plot C_e/q_e vs C_e. The constant k_f (L/mg) is an empirical constant of the Freundlich isotherm, while n indicates a value that is related to adsorption intensity (Rao, Ikram, & Ahmad, 2011).

The adsorption isotherm of Pb(II) on hydroxyapatite and hydroxyapatite-SiO_2 composites is shown in **Figures 8** and **9**. The correlation coefficient value (R^2) of the Langmuir isotherm is higher than Freundlich isotherm, showing that the Langmuir isotherm model is more appropriate for explaining the adsorption model of Pb(II) on hydroxyapatite and hydroxyapatite-SiO_2 composite. This model indicates the monolayer adsorption mechanism.

Table 2 shows the Langmuir and Freundlich parameters. The maximum adsorption capacity of the hydroxyapatite-SiO_2 composite is greater than hydroxyapatite. The addition of SiO_2 to hydroxyapatite increases the adsorption capacity. The silanol groups have a role in reducing Pb(II) from aqueous solution. The silanol group releases H^+ and forms SiO- which can adsorb Pb(II) (Hu, Wang, & Pan, 2010). The value of n between 1 and 10 represents favorable adsorption (Kalaivani et al., 2014). This study obtained n > 1 for both hydroxyapatite and hydroxyapatite-SiO_2 composite. Besides that, values of n between 1 and 10 describe beneficial adsorption (Rao et al., 2011).

The difference of maximum adsorption capacity using variations of adsorbent to removal Pb(II) is shown in **Table 3**. The hydroxyapatite and hydroxyapatite-SiO_2 composite have maximum adsorption capacity for Pb(II) are 123.46 and 135.14 mg/g, respectively. The maximum adsorption capacity is higher than the other adsorbents. The result shows that hydroxyapatite-SiO_2 composite can effectively use as an adsorbent of Pb(II).

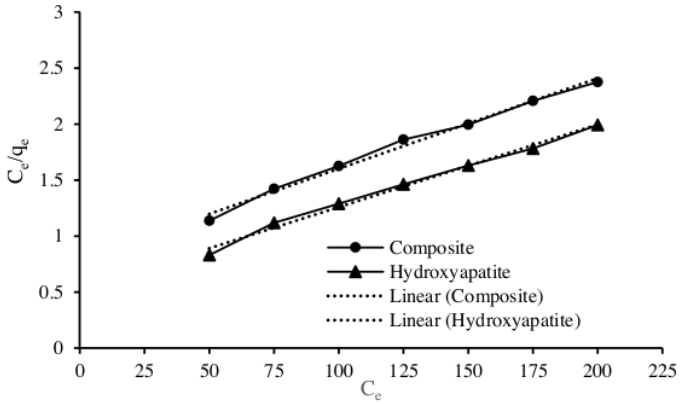

Figure 8. The Langmuir isotherm of Pb(II) onto hydroxyapatite and hydroxyapatite-SiO_2 composite

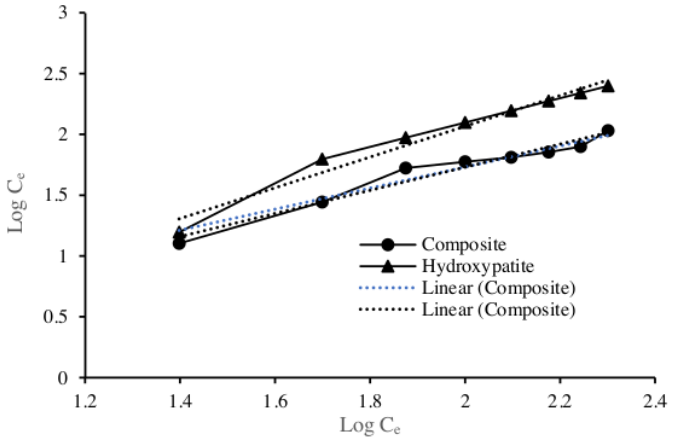

Figure 9. Freundlich isotherm of Pb(II) onto hydroxyapatite and hydroxyapatite-SiO_2 composite

Table 2. Isotherm parameters of Langmuir and Freundlich models for Pb(II) adsorption onto hydroxyapatite and hydroxyapatite-SiO_2 composite

Adsorbent	Langmuir isotherm			Freundlich isotherm		
	q_m	b	R^2	k_f	n	R^2
Hydroxyapatite	123.46	0.010	0.9918	2.900	1.052	0.9693
Hydroxyapatite-SiO_2 composite	135.14	0.014	0.9920	1.482	1.037	0.9622

Table 3. The difference of maximum adsorption capacity for Pb(II) by a various adsorbent

Adsorbent	q_m (mg/g)	Reference
Polystyrene-alumina activated carbon composite	22.47	Rao et al., (2011)
Acid modified montmorillonite	1.26	Akpomie & Dawodu (2016)
Oxidized multiwalled carbon nanotubes/polypyrrole composite	5.720	Nyairo et al., 2018
Hydroxyapatite synthetic	14.75	Le et al., 2019
Montmorillonite-K10	95.23	Humelnicu, Ignat, & Suchea, 2015
Al-pillared clay	97.08	Humelnicu et al., 2015
Activated carbon (from palm oil mill effluent)	114.28	Adebisi, 2017
Graphene oxide-montmorillonite	19.39	Zhang, Luan, Chen, Ke, & Zhang (2019)
Biochar from peanut shell	56.49	Tazar & Ozer (2020)
Hydroxyapatite	123.46	In this study
Hydroxyapatite-SiO_2 composite	135.14	In this study

Table 4. Kinetic parameters for adsorption Pb(II) onto hydroxyapatite and hydroxyapatite-SiO_2 composite

Kinetic parameters	Hydroxyapatite	Hydroxyapatite-SiO_2 composite
Pseudo-first order		
R^2	0.9492	0.9506
k_1 (1/min)	0.0011	0.0068
Pseudo-second order		
R^2	0.9934	0.9954
k_2 (g/mg.min)	0.0131	0.0138

Adsorption Kinetic

Adsorption kinetic models were studied to determine the mechanism of adsorption, control of adsorption steps such as chemical reactions, transport of mass, and kinetics adsorption (Rao et al., 2011). The pseudo-first-order and pseudo-second-order are used to describe kinetic models in this study. The equations are as follows:

$$\log (q_e - q_t) = \log q_e - \frac{k_1}{2.303} t \quad (3)$$

$$\frac{t}{q_t} = \frac{1}{k_2 q_e^2} + \frac{1}{q_e t} \quad (4)$$

q_e and q_t (mg/g) are the adsorption capacity at equilibrium and every time (t). k_1 and k_2 are the pseudo-first-order and pseudo-second-order adsorption rate constant. The value of *k* is determined from the slope and intercept of the plot of the equation at different times. As shown at **Table 4**, the pseudo-second-order is more suitable to describe the model of adsorption Pb(II) on hydroxyapatite and hydroxyapatite-SiO_2 composite. The correlation coefficient (R^2) of pseudo-second-order is greater than the pseudo-first-order.

CONCLUSIONS

In this study, hydroxyapatite was successfully synthesized from golden snail shells (*Pomacea canaliculata* L). The composite of hydroxyapatite and SiO_2 was made to remove Pb(II) from aqueous solution. The optimum adsorption process was obtained at pH solution 6 and 60 minutes of contact time using hydroxyapatite and hydroxyapatite-SiO_2 composites. Hydroxyapatite and hydroxyapatite-SiO_2 composite are potential to be used as adsorbents. The maximum adsorption capacity of both adsorbents is greater than several adsorbents. However, the hydroxyapatite-SiO_2 composite has a maximum adsorption capacity greater than hydroxyapatite. The adsorption process of the two adsorbents follows Langmuir isotherm at room temperature and also follows the pseudo-second-order kinetics.

ACKNOWLEDGMENTS

This study received financial support from Unggulan Kompetitif grant, Universitas Sriwijaya No. 0149.157/UN9/SB3.LP2M.PT/2019.

REFERENCES

Adebisi, G. A., Chowdhury, Z. Z., & Alaba, P.A. (2017). Equilibrium, kinetics, and thermodynamics studies of lead ion and zinc ion adsorption from aqueous solution onto activated carbon prepared from palm oil mill effluent. *Journal of Clean Production*, 148, 958-968.

Apokmie, K.G., & Dawodu, F. A. (2016). Acid modified montmorillonite for sorption of heavy metals from automobile effluent. *Beni-Suef University Journal of Basic and Applied Sciences*, 5, 1-12.

Balamurugan, A., Kannan, S., & Rajeswari, S. (2002). Synthesis of hydroxyapatite on silica gel surface by using glycerin as a drying control chemical additive. *Materials Letters*, 57, 1244-1250.

Campbell, N. A., Reece, J. B., & Mitchell, L. G. (2005). Biology. 5 th edition. Benjamin-Cummings Pub. Co.

Dhmees, A. S., Khaleel, N. M., & Mahmoud, S.A. (2018). Synthesis of silica nanoparticles from blast furnace slag as cost-effective adsorbent for efficient azo-dye removal. *Egyptian Journal of Petroleum*, 27, 1113-1121.

Dong, L., Zhu, Z., Qiu, Y, & Zhao, J. (2010). Removal of lead from aqueous solution by hydroxyapatite/magnetite composite adsorbent. *Chemical Engineering Journal*, 165, 827-834.

Dong, L., Zhu, Z., Qiu, Y., & Zhao, J. (2016). Removal of lead from aqueous solution by hydroxyapatite/manganese dioxide composite. *Frontiers Environmental Science & Engineering*. 10, 28-36.

Esmaelkhanian, A., Sharifianjazi, F., Abouchenari, A., Rouhani, A., Parvin, N., & Irani, M. (2019). Synthesis and characterization of natural nano-hydroxyapatite derived from Turkey Femur-Bone Waste. *Applied Biochemistry and Biotechnology*, 189, 919-932.

Farghali, A. A., Bahgat, M., Allah, A. E., & Khedr, M. H. (2013). Adsorption of Pb(II) ions from aqueous solutions using copper oxide nanostructure. *Beni-Suef University Journal of Basic and Applied Sciences*, 2, 61-71.

Ferreira, C. S., Santos, P. L., Bonacin, J. A., Passos, R. R., & Pocrifka, L. A. (2015). Rice house reuce in the preparation of SnO_2/SiO_2 nanocomposite. *Materials Research*, 18, 639-643.

Gu, S., Wang, L., Mao, X., Yang, L., & Wang, C. (2018). Selective adsorption of Pb(II) from aqueous solution by triethylenetetramine-grafted polyacrylamide/vermiculite. *Materials*, 11, 1-20.

Hajdu, I., Bodnar, M., Csikos, Z., Wei, S., Daroczi, L., Kovacs, B., Gyori, Z., Tamas, J., & Barbely, J. (2012). Combined nano-membrane technology for removal of lead ions. *Journal of Membrane Science*, 409-410, 44-53.

Hassan, M. A., Mohammed, A. M., Salaheldin, T. A., & El-Anadouli, B. E. (2018). A promising hydroxyapatite/graphene hybrid nanocomposite for methylene blue dye's removal in wastewater treatment. *International Journal of Electrochemical Science*. 13, 8222-8240.

Hariani, P. L., Muryati, Said, M. (2019). Kinetic and thermodynamic adsorption of nickel (II) onto hydroxyapatite prepare from snakehead (*Channa striata*) fish bone. *Mediterranean Journal of Chemistry*, 9, 85-94.

He, Y., Wu, P., Xiao, W., Li, G., Yi, J., Chen, C., Ding, P., & Duan, Y. (2019). Efficient removal of Pb(II) from aqueous solution by a novel ion impreted magnetic biosorbent: Adsorption kinetics and mechanisms. *Plos One*, 14, 1-17.

Hu, H., Wang, Z., & Pan, L. (2010). Synthesis of monodisperse Fe_3O_4@silica core-shell microspheres and their application for removal of heavy metal ions from water. *Journal of Alloy and Compounds*, 492, 656-661.

Humelnicu, D., Ignat, M., & Suchea, M. (2015). Evaluation of adsorption capacity of montmorillonite and aluminium-pillared clay for Pb^{2+}, Cu^{2+} and Zn^{2+}. *Acta Chimica Slovenica,* 62, 947-957.

Iconaru, S, L., Heino, M. M., Guegan, R., & Predoi, M. V. (2018). Removal of zinc ions using hydroxyapatite and study of ultrasound behavior of aqueous media. *Materials*, 11, 1-16.

Jain, M., Yadav, M., Kohout, T., Lahtinen, M., Kumar, V. K., & Sillanpaa, M. Development of iron oxide/activated carbon nanopartcle composite for the removal of Cr(VI), Cu(II) and Cd(II) ions from aqueous solution. (2018). *Water Resources and Industry*, 20, 54-74.

Jarup, L. (2003). Hazards of heavy metal contamination. *British Medical Bulletin*, 68, 167-182.

Kalaivani, S. S., Vidyadevi, T., Murugesan, A., Baskaralingam, P., Anuradha, C. D., Ravukumar, R., & Sivanesan, R. (2014). Equilibrium and kinetics studies on the adsorption of Ni(II) ion from aqueous solution using activated carbon prepared from Theobroma cacao (cocoa) shell. *Desalination and Water Treatment*, 54, 1629-1641.

Kausar, A., Naeem, K., Hussain, T., Nazli, Z., Bhatti, H. N., Jubeen, F., Nazir, A., & Igbal N. (2019). Preparation and characterization of chitosan/clay composite for direct Rose FRN dyr removal from aqueous media: comparison of linear and non-linear regresion methods. *Journal of Materials Research and Technology*, 8, 1161-1174.

Kavak, D. (2013). Removal of lead from aqueous solution by precipitation: statistical analysis and modeling. *Desalination and Water Treatment,* 51, 1720-1726.

Latifi, S. M., Fathi, M. H., & Golozar, M. A. (2012). Preparation and characterization of hydroxyapatite-silica composite nanopowders. In *International Journal of Modern Physics: Conference Series* (Vol. 5, p. 630). World Scientific Publishing Company.

Le, D. T., Le, T. P. T., Do, H. T., Yo, H. T., Pham , N. T., Nguyen, T. T., Cao, H. T., Nguyen, P. T., Dinh, T. M. T., Le, H. V., Tran, L. D. (2019). Fabrication of porous hydroxyapatite granules as an effective adsorbent for the removal of aqueous Pb(II) ions. *Journal of Chemistry*, 2019, 1-11.

Li, X., Li, H., Xu, X., Guo, N., Yuan, L., & Yu, H. (2017). Preparation of a reduce graphene oxide @stainless steel net electrode and its application of electrochemical removal Pb(II). *Journal of The Electrochemical Society*, 164, 71-77.

Lin, K., Pan, J., Chen, Y., Cheng, R., & Xu, X. (2009). Study the adsorption of phenol from aqueous solution on hydroxyapatite nanopowders. *Journal of Hazardous Materials*, 161, 231-240.

Meyers, P., Gottlieb, L., DeSilva, F. (2013). Lead removal by ion exchange. John Wiley and Sons, Inc. Hoboken.

Miecznik, J. B., Haberko, K., Sitarz, M., Bucko, M. M., Macherzynska. (2014). Hydroxyapatite from animal bones-extraction and properties. *Ceramics International*, 41, 4841-4846.

Music, S., Vincekovic, F., & Sekovanic, L. (2011). Precipitation of amorphous SiO_2 particles and their properties. *Brazilian Journal of Chemical Engineering*, 28, 89-94.

Nyairo, W. N., Eker, Y. R., Kowenje, C., Akin, I., Bingol, H., & Ongeri, D. M. (2018). Efficient adsorption of lead (II) and copper (II) from aqueous phase using oxidized multiwalled carbon nanotubes/polypyrrole composite. *Separation Science and Technology*, 53(10), 1498-1510.

Parida, S. K., Dash, S., Patel, S., & Mishra, B. K. (2006). Adsorption of organic molecules on silica surface. *Advances in Colloid and Interfaces Sciences*, 121, 77-110.

Ragab, A., Ahmed, I., & Bader, D. (2018). The removal of brilliant green dye for aqueous solution using nanohydroxyapatite/chitosan composite as a sorbent. *Molecules*, 24, 1-16.

Ramesh, S. T., Rameshbabu, N., Gandhimathi, R., Nidheesh, P. V., & Kumar, M. S. (2012). Kinetics and equilibrium studies for the removal of heavy metals in both single and binary system using hydroxyapatite. *Applied Water Science*, 2, 187-197.

Rao, R. A. K., Ikram, S., & Ahmad, J. (2011). Adsorption of Pb(II) on a composite material prepared from polystyrene-alumina and activated carbon: kinetic and thermodynamic studies. *Journal of The Iranian Chemical Society*, 8(4), 931-943.

Samuel, M. S., Shah, S.S., Bhattacharya, J., Subramaniam, K., & Singh, N. D. P. (2018). Adsorption of Pb(II) from aqueous solution using a magnetic chitosan/graphene oxide composite and its toxicity studies. *International Journal of Biological Macromolecules*, 115, 1142-1150.

Sayari, A., Hamoudi, S., & Yang, Y. (2005). Applications of pore-expanded silica. 1. Removal of heavy metal cations and organics pollutants from wastewater. *Chemistry of Materials*, 17, 212-216.

Skwarek, E. (2014). Adsorption of Zn on synthetic hydroxyapatite from aqueous solution. *Separation Science and Technology*, 49, 1654-1662.

Sunil, B. R., & Jagannatham. (2016). Producing hydroxyapatite from fish bone by heat treatment. *Materials Letters*, 185, 411-414.

Tasar, S., & Ozer, A. (2020). A thermodynamic and kinetic evaluation of the adsorption of Pb(II) ions using peanut *(Arachis Hypogaea)* shell-based biochar from aqueous media. *Polish Journal of Environmental Studies*, 29(1), 293-305.

Tawinteung, N., Parkpian, P., Delaune, R. D., & Jugsujinda, A. (2005). Evaluation of extraction procedures for removing lead from contaminated soil. *Journal of Environmental Science and Health*, 40, 385-407.

Wu, S. C., Hsu, H. C., Hsu, S. K., Chang, Y. C., & Ho, W. F. (2016). Synthesis of hydroxyapatite from eggshell powder through ball milling and heat treatment. *Journal of Asean Ceramic Societies*, 4, 85-90.

Widiyastuti, W., Machmudah, S., Nurtono, T., Winardi, S., & Okuyama, K. (2017). Synthesis of Zn-SiO_2 nanocomposite particles and their characterization by sonochemical method. In *AIP Conference Proceedings* (Vol. 1840, p. 0800081). AIP Publishing.

Xu, D., Tan, X., Chen, C., & Wang, X. (2008). Removal of Pb(II) from aqueous solution by oxidized multiwalled carbon nanotubes. *Journal of Hazardous Materials*, 154, 407-416.

Zhang, C., Luan, L., Chen, W., Ke, X., & Zhang, H. (2019). Preparation of graphene oxide-montmorillonite nanocomposite and its application in multiple-pollutants removal from aqueous solutions. *Water Science and Technology*, 79(2), 323-333.

Removal of pb(II)

ORIGINALITY REPORT

23%	12%	17%	7%
SIMILARITY INDEX	INTERNET SOURCES	PUBLICATIONS	STUDENT PAPERS

MATCH ALL SOURCES (ONLY SELECTED SOURCE PRINTED)

1%

★ M.L. Montes, F. Barraqué, A.L. Bursztyn Fuentes, M.A. Taylor, R.C. Mercader, J. Miehé-Brendlé, R.M. Torres Sánchez. "Effect of synthetic beidellite structural characteristics on the properties of beidellite/Fe oxides magnetic composites as Sr and Cs adsorbent materials", Materials Chemistry and Physics, 2020

Publication

Exclude quotes	Off	Exclude matches	Off
Exclude bibliography	Off		